Fast Quasi-Flat Zones Filtering Using Area Threshold and Region Merging

J. Weber[a,*], S. Lefèvre[b]

[a] *Université de Lorraine, LORIA-UMR 7503, France*
[b] *Université de Bretagne Sud, IRISA, France*

Abstract

Quasi-flat zones are morphological operators which segment the image into homogeneous regions according to certain criteria. They are used as an image simplification tool or an image segmentation pre-processing, but they induced a very important oversegmentation. Several filtering methods have been proposed to deal with this issue but they suffer from different drawbacks, e.g., loss of quality or edge deformation. In this article, we propose a new method based on existing approaches which achieves better or similar results than existing approaches, does not suffer from their drawbacks and requires less computation time. It consists of two successive steps. First, small quasi-flat zones are removed according to a minimal area threshold. They are then filled through the growth of remaining zones.

Keywords: Quasi-flat zones, Mathematical Morphology, Quasi-Flat Zones Filtering, Image Segmentation

*Corresponding author.
Phone: +33 (0) 329.536.041.
Address: LORIA Nancy, Campus Scientifique - BP 239, 54506 Vandœuvre-les-Nancy Cedex, France
Email addresses: jonathan.weber@loria.fr (J. Weber), sebastien.lefevre@univ-ubs.fr (S. Lefèvre)

1. Introduction

Quasi-flat zones are morphological operators which partition the image into homogeneous regions according to certain criteria. They are mainly used for image simplification and image segmentation (through a pre-processing). However quasi-flat zones induce a very important oversegmentation which is mostly due to tiny quasi-flat zones composed of a few pixels. As these small regions do not improve the quality of the QFZ partition, several methods have been proposed to filter them. These methods reduce the oversegmentation but suffer from different drawbacks : loss of quality, edge deformation, etc. So, there is still a need of an efficient method for quasi-flat zones filtering. Here, we propose such a method by inspiring from existing approaches while achieving better or similar results, not suffering from the known drawbacks and requiring a lower computation time. It consists of two successive steps. First, small quasi-flat zones are removed according to a minimal area threshold. They are then filled through the growth of remaining zones. This paper is organized as follows. In the next section, we present the paradigm of quasi-flat zones, their applications to image analysis and processing, and their related issues. Sec. 3 is dedicated to a early introduction of the evaluation protocol which will be used thorough our paper. We then given an overview of the state-of-the-art in Sec. 4. In Sec. 5, we introduce our proposal which outperforms current approaches as shown by the experiments in Sec. 6. We finally conclude in Sec. 7 and indicate some future directions.

2. Background

2.1. Quasi-Flat Zones

Flat zones [10] have been studied within the field of Mathematical Morphology and are seen as elements with interesting properties. Indeed, a flat zone is defined as a connected set of pixels having the same value. Since object frontiers in digital images are mostly located between pixels of different values, object frontiers are expected to be included in frontiers between flat zones. However,

flat zones are often only a few pixels wide so the resulting partition is an extreme oversegmentation and is hardly exploitable. Less constrained definitions have thus been proposed, leading for instance to the Quasi-Flat Zones (QFZ) and more precisely the C^α (see [12] for a survey on QFZ).

The C^α of a pixel p is defined as the connected set of pixels which can be reached through (at least) one path verifying the following condition: the difference between values of successive pixels within the path is less or equal to a given parameter α ($\alpha = 0$ being the case of flat zones). However, segmenting an image into C^α with $\alpha > 0$ may result in an undersegmentation phenomenon. If α is set too high, it will lead to a so-called chaining effect, which may even result in a single QFZ for the whole image. In order to counter this problem, several new QFZ definitions based on C^α have been elaborated (see [12] for more details). These definitions have been subsequently unified by Soille and Grazzini [11, 14], who propose a theoretical framework called logical predicate connectivity.

In this new framework, a QFZ (noted $C^{P_1,\ldots,P_n}$ here) is expected to satisfy all the n logical predicates P_i. We will denote by $P_i(S)$ the fact that a predicate P_i is valid over a set S. Various predicates may be involved, such as the global range predicate which is true if and only if the difference between minimal and maximal pixel values within a QFZ is less or equal to a given threshold ω. The $C^{P_1,\ldots,P_n}$ thus consists in finding, for each pixel p, the largest C^α which satisfies all the predicates. Moreover, since the following property holds:

$$\forall \alpha' \leq \alpha, \qquad C^{\alpha'}(p) \subseteq C^\alpha(p) \tag{1}$$

an iterative computation scheme may be involved. Indeed, when predicates are not verified for a given value of α, α is decremented and a new evaluation of the predicates is performed. This loop is repeated until finding the maximal value of α for which all the predicates are verified:

$$C^{P_1,\ldots,P_n}(p) = \bigvee \left\{ C^{\alpha'}(p) \;\middle|\; \begin{array}{l} \forall k \in \{1,\ldots,n\},\ \forall \alpha'' \leq \alpha',\ \forall q \in C^{\alpha'}(p) \\ P_k\left(C^{\alpha'}(p)\right) = \textbf{true} \text{ and } P_k\left(C^{\alpha''}(q)\right) = \textbf{true} \end{array} \right\} \tag{2}$$

In the following we will use C^{α} which only relies on local range predicate α, and $C^{\alpha,\omega}$ which relies on both local range predicate α and global range predicate ω.

Some clues to define QFZ in multivariate images have also been given by Soille [12], where α is assumed to be a vector with the same value in all components. Thus α may be easily ordered through a total ordering (e.g., decrementing $\alpha = (3,3,3)$ gives $\alpha = (2,2,2)$). Global range predicate is processed similarly, and is true only if it is verified marginally for all bands.

2.2. QFZ-based image analysis

Quasi-flat zones are mainly used as an image simplification tool and as a first step within a segmentation process.

In the context of image simplification, QFZ are interesting since they produce connected sets of homogenous pixels (according to a certain criterion). The key idea is to set a unique intensity value for all pixels belonging to the same quasi-flat zone, for instance its mean intensity [12]. Other works aim at not only spectrally simplifying the image but also simplifying shapes in the image to ease its subsequent vectorization [4]. Such image simplifications are used for compression purpose or image filtering before segmentation.

Indeed, quasi-flat zones can also be considered as a first segmentation step. The resulting partition can then be refined by merging close and similar quasi-flat zones [3] or using representative quasi-flat zones as seeds in a seeded segmentation process like watershed [17] or seeded region merging [6]. They have also been used to speed up interactive video segmentation [15], by considering quasi-flat zones instead of pixels as partition elements.

In this article, we will deal with this last application case and consider quasi-flat zones from a segmentation point-of-view.

2.3. The case of transition regions and isolated pixels

All QFZ definitions suffer from the transition region problem. These regions are border regions between two objects where there is a stair effect (cf. Fig. 1.b). This effect is due to the image discretization and the interpolation of pixel values induced. It leads to an oversegmentation close to this border which is then composed of tiny QFZ (cf. Fig. 1.c).

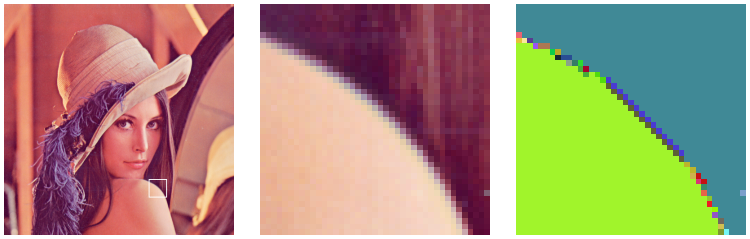

a *b* *c*

Figure 1: Transition region problem: a) original image, b) Stair effect in the white square of the original image, c) $C^{\alpha,\omega}$ using $\alpha = \omega = 100$.

This local oversegmentation might be very important and needs to be lowered in order the QFZ partition to be meaningful. This can be achieved without any loss of quality in the resulting segmentation since the oversegmented areas of the image are located on the border between objects.

Transition regions are not the only cause of oversegmentation. In fact, they account only for those on contrasted borders (see Fig. 1 where transition regions are located between the light shoulder of Lenna and her dark hairs). Indeed, we may also observe numerous QFZ made of a single pixel inserted in a wider QFZ (see Fig. 2). These QFZ are due to isolated pixels (pixels surrounded by a homogeneous neighbourhood). Such QFZ are not useful for image segmentation or simplification, and must be filtered. Moreover, we can also observe that there are regions which are segmented into too many QFZ (for instance Lenna shoulder in Fig. 2, whatever the values of the parameters α and ω considered). It is obviously necessary to filter these regions to keep oversegmentation reduced and thus still useful.

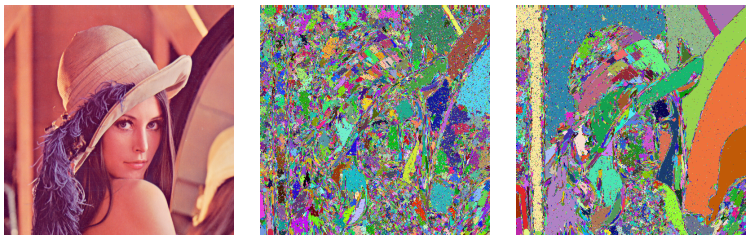

a *b* *c*

Figure 2: Oversegmentation on *lenna* : a) Original image, b) $C^{\alpha,\omega}$ using $\alpha = \omega = 50$ (58,219 QFZ), c) $C^{\alpha,\omega}$ using $\alpha = \omega = 100$ (34,651 QFZ).

To achieve oversegmentation reduction, dedicated filtering methods are required to specifically address small QFZ and transition regions. Before reviewing these methods, we deal in the next section with the problem of their evaluation.

3. Evaluation protocol

Before describing quasi-flat zone filtering methods in the following sections, we introduce our evaluation protocol which will be used thorough our paper to compare the different methods.

We have considered here the Berkeley Segmentation Dataset [8]. It contains 300 color images of size 481×321 pixels and 3269 reference segmentations, realized by 28 distinct experts. The relatively high number of reference segmentation maps per image is significant in the context of our experiments. Indeed, it enables a more objective comparison between our results and real-world practical requirements. A sample of the collection along with reference segmentation maps is provided in Fig. 3.

The comparison between filtering methods is achieved quantitatively by means of a segmentation task. Segmentation being an ill-posed problem, its evaluation is still an issue (multiple ground truths are possible depending on the expert involved). Simple criteria as the number of regions is definitely insufficient. In order to strengthen the objectivity of the experiment under consideration, we thus employ here two evaluation criteria: the oversegmentation

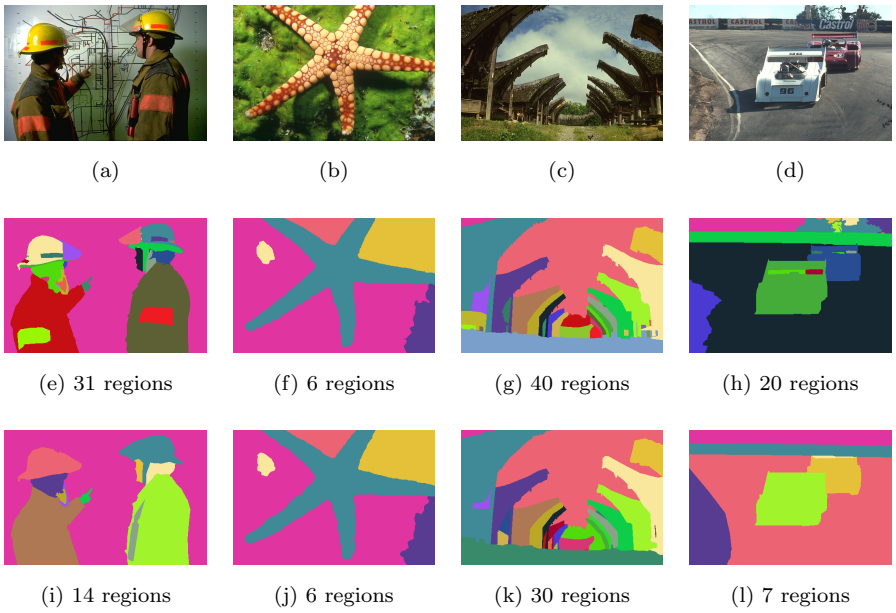

(a) (b) (c) (d)

(e) 31 regions (f) 6 regions (g) 40 regions (h) 20 regions

(i) 14 regions (j) 6 regions (k) 30 regions (l) 7 regions

Figure 3: Images from the Berkeley Segmentation Dataset: the original images (top) along with two reference segmentation maps (middle and bottom).

ratio (OSR) [5] and maximal precision (MP) [7]. The former is defined as:

$$OSR = \frac{\#\text{ quasi-flat zones}}{\#\text{ reference regions}} \tag{3}$$

This ratio directly expresses the degree of over-segmentation. It provides us somehow with the merging degree required to achieve a segmentation as closest to the reference as possible.

The latter rather focuses on pixel-based accuracy by comparing the reference segmentation and the built quasi-flat zones. More precisely, each quasi-flat zone is associated with a given reference region for which it shares the highest number of pixels. It results in the best possible segmentation we can obtain by an optimal merging of QFZ. We then measure a pixel-based precision by computing the ratio of well-segmented pixels:

$$MP = \frac{\#\text{ well-segmented pixels}}{\text{total }\#\text{ pixels}} \tag{4}$$

For instance, $MP = 0.8$ means that we have achieved 80% pixel-based accuracy

w.r.t. the ground-truth. Hence, by using both MP and OSR, an effective evaluation and comparison might be achieved, with the ultimate goal being both the minimization of OSR and maximization of MP.

Having established OSR and MP as evaluation criteria, we proceeded to apply various quasi-flat zone filtering methods on the entire Berkeley Dataset (cf. Fig. 8). Multiple references for each image are used individually for evaluation and combined to obtain a mean evaluation for each image. The plotted results are the mean of the evaluations obtained on the whole dataset.

4. Comprehensive review of related work

Several approaches have been proposed to deal with the problems of transition regions and isolated pixels. The goal of this section is to provide a comprehensive review of these methods.

Soille and Grazzini [14] define the transition regions as QFZ that contain only transition pixels. A transition pixel is a pixel which is not a local extremum, i.e. which is not surrounded by either lower or higher values only.

The approach proposed by Soille and Grazzini consists in removing all the QFZ which are transition regions, i.e. regions without local extremum. The resulting incomplete image partition is then corrected by using a region-merging algorithm (here the Seeded Region Growing (SRG) [1]). The remaining QFZ are used as seeds and grow until the partition of the image is complete. The authors also proposed an extension of their approach dedicated to color images. The key idea is to consider that a pixel is a transition pixel only if it is a transition pixel in every color band of the image.

Fig. 4 illustrates this approach both in grayscale and color case, and provides final as well as intermediary results. Amounts of QFZ are heavily reduced (60.7% in grayscale and 36.8% in color) but the oversegmentation is still important after the filtering of transition regions. While transition pixels account for most of the image pixels, transition regions represent only a much smaller part of the image because of their strict definition. In fact, local extrema, even if fewer

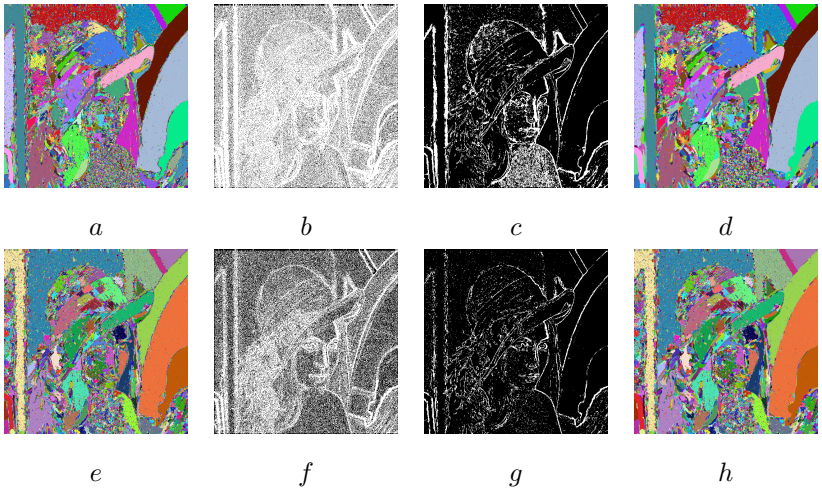

Figure 4: Transition region filtering : (top) grayscale, a) $C^{\alpha,\omega}$ using $\alpha = \omega = 100$ (31,385 QFZ), b) Transition pixels mask (82% of the image), c) Transition region mask (19 073 transition regions representing 17% of the image), d) QFZ after filtering (12,313 QFZ); (bottom) color, e) $C^{\alpha,\omega}$ using $\alpha = \omega = 100$ (34,651 QFZ), f) Transition pixels mask (57% of the image), g) Transition region mask (12,743 transition regions representing 9% of the image), h) QFZ after filtering (21,909 QFZ).

than transition pixels, are well distributed in the image. Due to the stricter definition of color transition pixels, we can observe the difference between color and greyscale transition regions. This approach does not need any parameter thanks to a precise definition of transition region. However, many regions made of few pixels remain after the transition region filtering. These regions do not fit the transition region definition but induce an important oversegmentation, as noticed in Sec. 2.3.

Soille [13] proposed a preprocessing of the original image instead of a postprocessing of the QFZ. This preprocessing consists in an image contrast reinforcement based on local extrema. First, local extrema of the image are extracted (cf. Fig. 5.a). Then, these extrema are used as seeds in a region growing process in order to obtain a partition of the image called *mosaic of local extrema* (cf. Fig. 5.b). Each pixel is then valued by the value of the local extremum used as seed for its region. This leads to a new image which contrast has been reinforced (cf Fig. 5.c). This preprocessing strengthens the edges in the image thus limiting the stair effect responsible of the majority of transition regions. Finally, QFZ are built from this image (cf Fig. 5.d).

a *b* *c* *d*

Figure 5: Filtering by local extrema mosaic: a) local extrema mask (43% of the image), b) local extrema mosaic (112,461 regions), c) original image with reinforced contrast, d) $C^{\alpha,\omega}$ using $\alpha = \omega = 100$ on reinforced contrast image (8,045 regions).

The filtering by local extrema mosaic induces an image simplification which let the subsequent QFZ partition to be far less oversegmented. However, we can still notice numerous QFZ made of a single pixel which prevent the overseg-

mentation to be considered as acceptable. Moreover, the contrast reinforcement modifies the edges of the processed image. This can be observed on the edges of Lenna's mirror (cf. Fig. 2 and 5.d). This modification has a direct impact on the quality of the QFZ partition in terms of boundary accuracy.

To accurately deal with isolated pixels, some authors have introduced filtering methods based on a minimal area threshold. Angulo [2] proposed to merge QFZ with an area lower than a threshold. QFZ are mapped to a region adjacency graph (RAG) where nodes represent QFZ and are valued by their mean color and area. Every vertex represents the adjacency link between two QFZ and is valued by the difference of mean colors of these two QFZ. The filtering proceeds by reducing this graph until all remaining QFZ have an area greater or equal to the threshold. The merging process is the following : the smallest QFZ is merged with the most chromatically similar adjacent QFZ, then the RAG is updated (node and vertex values). This process is repeated until no QFZ has an area lower than the minimal area threshold. Even a small threshold value leads to removing few pixels QFZ and transition regions. However, as small QFZ are merged with adjacent QFZ, it is possible that these adjacent QFZ are also small QFZ and then, the filtering can produce QFZ greater than the threshold but only composed of small QFZ such as transition regions (cf. Fig. 6). Since boundaries are generally present in such QFZ (especially transition regions), it might alleviate the partition accuracy.

Zanoguera [17] proposed an approach based on a similar principle. It also aims at removing QFZ with an area lower than a given threshold. To obtain a complete partition of the image, remaining QFZ are used as markers for marker-based watershed algorithm [9]. These QFZ are then extended in the space from which small QFZ have been removed. Contrary to Angulo's approach, there is no risk to obtain QFZ only composed of transition regions. However, the watershed is applied on pixels, so the removed QFZ information and the data reduction they induce are lost. It calls for an improvement by applying watershed on QFZ instead of pixels. Such an extension would preserve QFZ information (particularly their accurate boundaries) and speedup the filtering

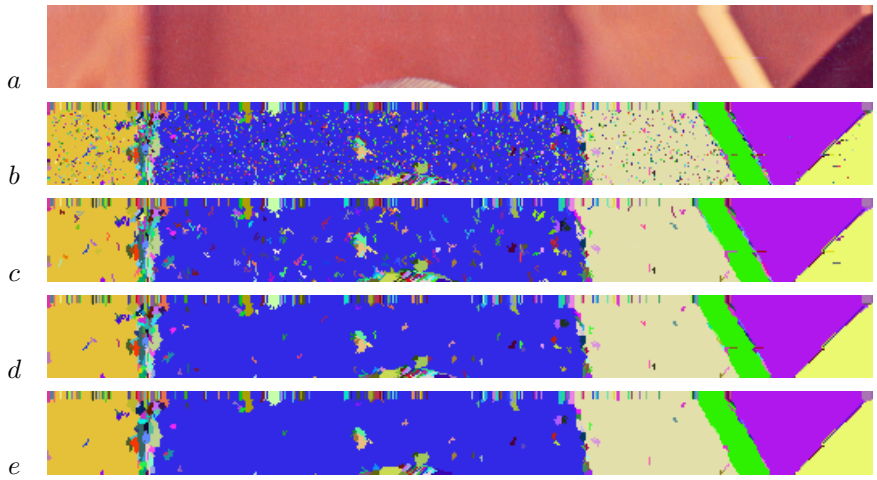

Figure 6: Enlargement of small QFZ after filtering on magnified top of *lenna*. a) original, b) $C^{\alpha,\omega}$ with $\alpha = \omega = 100$, c) Angulo's method (area threshold = 5), d) Iterative area filtering (area threshold = 5), e) Zanoguera's method (area threshold = 5) (no small QFZ enlargement).

by working on the reduced data.

Crespo *et al.* [6] dealed with flat zones. The idea is to select the n most significant flat zones (depending to some criteria) as seeds in a region growing process applied on flat zones. Thus a precise over-segmentation reduction is obtained as the desired number of remaining flat zones has to be set. Moreover, the region growing is not applied on pixels but rather on flat zones. This ensures to keep accurate borders from flat zones and to limit computation cost since the region growing algorithm is applied on a reduced data volume. This method may be adapted to QFZ, but the parameter n is rather hard to be set since it is strongly image dependent.

Brunner and Soille [4, 13] proposed an iterative area filtering method. Similarly to previous methods, it aims at removing QFZ with area lower than a threshold. However, instead of removing all these QFZ in a single step, the removal is done by iteratively increasing the area threshold until the final threshold:

1. Area threshold is set to 2;
2. QFZ with area lower than the threshold are removed;
3. Partition is completed using remaining QFZ as seeds in a SRG algorithm;
4. If the current area threshold is not the final threshold, it is increased and the process go back to step 2, otherwise the filtering is achieved.

Since filtering is progressive, it avoids poor results induced by the fact that remaining QFZ (i.e. larger than the threshold) represent a small part of the image in case of a high threshold value. This approach thus filters few pixel QFZ and transition regions, but is also able to significantly reduce the over-segmentation when considering a high threshold value. In our example, we observe on Fig. 7 that the over-segmentation is further reduced w.r.t. other methods. However, we can notice that all transition regions have not been removed. Indeed, some have been enlarged by integrating pixels from removed QFZ and thus having an area greater than the final threshold. This leads to the production of transition regions wider than the original region transitions, while their filtering was expected (cf. Fig. 6). Moreover, the region growing process is applied on pixels: as it has been suggested for the previous method, applying such a process directly on QFZ looks more relevant.

Existing QFZ filtering approaches allow to reduce the important oversegmentation induced by QFZ. However, the oversegmentation is still high especially with non-parametric methods which mainly aim at filtering transition regions. Filtering approaches based on minimal area threshold reduce more efficiently the oversegmentation effect. Nevertheless, these approaches also suffer from some drawbacks: transition regions may be enlarged by aggregating small QFZ or parts of them, small QFZ may be removed while loosing their related information and the data compression power. Moreover, a minimal area threshold has to be set. Its value depends on the image content. In the case of an image with a wide (resp. small) object of interest, the threshold should be set high (resp. low). This is is illustrated in Fig. 8 where we can observe that the parametric approaches (iterative area filtering, Angulo's and Zanoguera's methods)

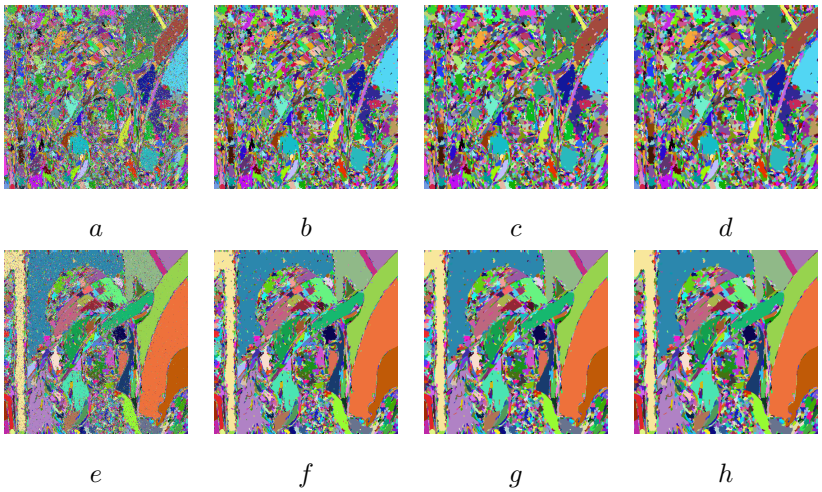

Figure 7: Iterative area filtering with $C^{\alpha,\omega}$: (top) $\alpha = \omega = 50$ a) non-filtered QFZ (58,219 QFZ), b) threshold=5 (11,423 QFZ), c) threshold=10 (6,335 QFZ), d) threshold=15 (4,528 QFZ), (bottom) $\alpha = \omega = 100$ e) non-filtered QFZ (34,651 QFZ), f) threshold=5 (6,381 QFZ), g) threshold=10 (3,386 QFZ), h) threshold=15 (2,411 QFZ).

lead to a greater oversegmentation reduction. Nonetheless, we also notice that a improving the oversegmentation reduction through the use of a higher threshold often comes at the cost of a lower maximal precision (cf. Fig. 9). So the threshold has to be set carefully and this is far from being trivial. We address these various issues in the next section.

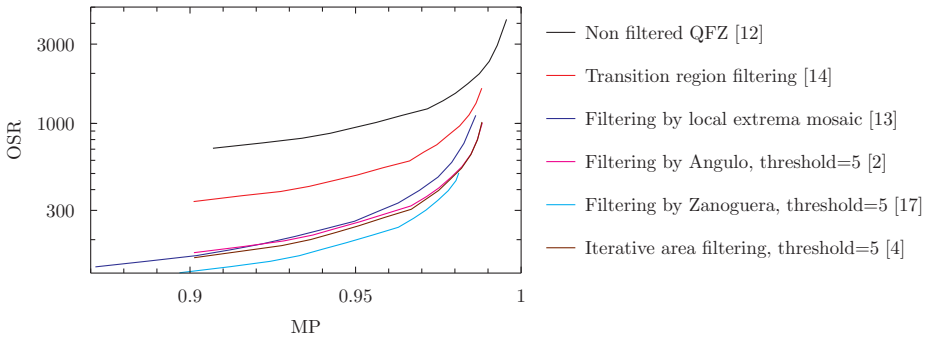

Figure 8: Existing QFZ filtering approaches comparison using $C^{(\alpha,\omega)}$ on Berkeley Segmentation Dataset.

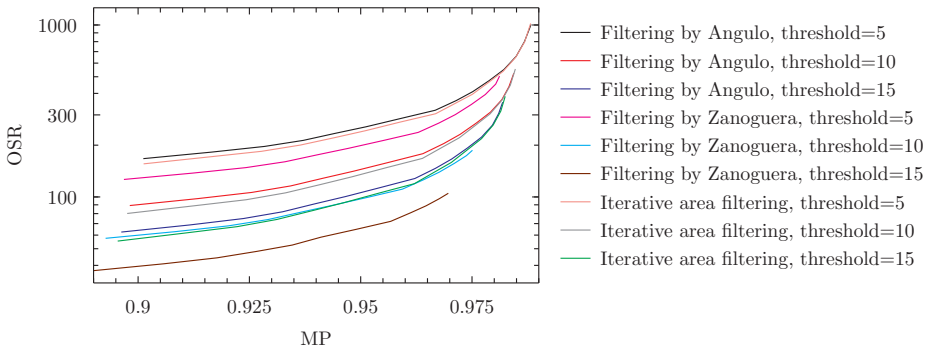

Figure 9: Filtering approaches based on minimal area threshold comparison using $C^{(\alpha,\omega)}$ on Berkeley Segmentation Dataset with different values of minimal area threshold.

5. Proposed method

In this section, we propose an original approach for QFZ filtering called *area filtering by merging*. We also evaluate the interest of working on QFZ rather than on pixels, give some clues to set the area threshold more easily and finally discuss the drawbacks and the advantages of our approach w.r.t. the state-of-the-art.

5.1. Definition

While failing to achieve accurate and effective oversegmentation reduction, existing approaches bring relevant features which are worth being considered. Thus we also consider the use of an area threshold. A merging process is also considered, thus leading to a 2-step approach:

(1) Removal of QFZ which area is less to the area threshold;

(2) Growing of the remaining QFZ using a SRG on the removed QFZ.

Instead of applying the partition completion on pixels, we apply it on QFZ in order to keep related information. Thus, the SRG is applied on the reduced data made from QFZ.

Fig. 10 illustrates the filtering process. Here QFZ are represented by mean colors of their pixels (Fig. 10.a). Small QFZ are removed but their spatial definition (i.e. the covered pixels) and mean color are kept (cf Fig. 10.b, removal of QFZ 3, 4 and 5). The SRG algorithm is then applied directly on QFZ using remaining QFZ as seeds (cf Fig. 10.c-e). At the end of the filtering process, remaining QFZ represent a complete image partition.

Fig. 11 illustrates our filtering approach applied on $C^{(\alpha,\omega)}$. The oversegmentation is greatly reduced even with small area threshold values. Compared to iterative area filtering results (Fig. 7), we observe that our method reduces more significantly the oversegmentation. Indeed, our approach does not face the problem of iterated QFZ aggregation stated in Sec. 4. In case of high threshold values, our method may induce some undersegmentation of some parts of the

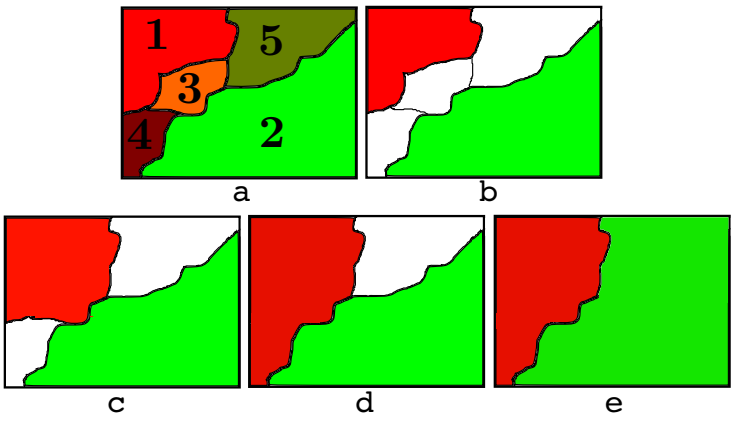

Figure 10: QFZ area filtering by merging : a) original QFZ, b) Removal of QFZ which area is less to the area threshold, c) first SRG iteration: QFZ 1 $\supset$ QFZ 3, d) second SRG iteration: QFZ 1 $\supset$ QFZ 4, e) last SRG iteration: QFZ 2 $\supset$ QFZ 5.

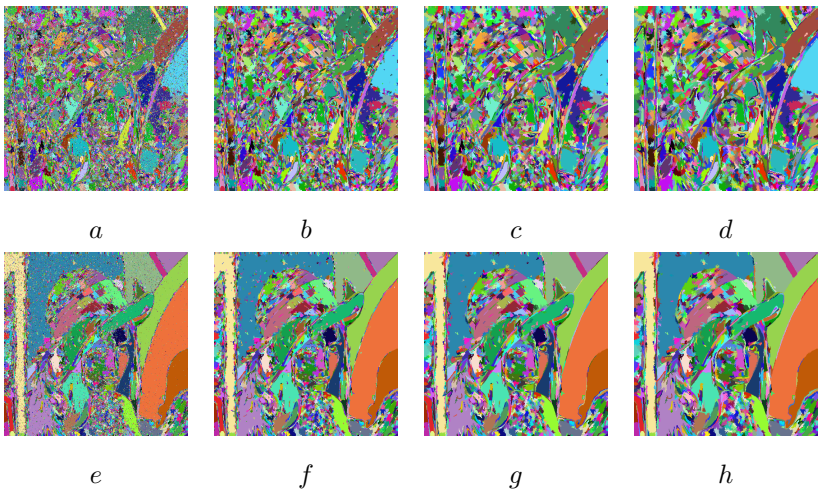

Figure 11: QFZ area filtering by merging on $C^{(\alpha,\omega)}$: (top) $\alpha = \omega = 50$; a) original QFZ (58, 219 QFZ); b) area threshold=5 (8, 014 QFZ); c) area threshold=10 (3, 572 QFZ); d) area threshold=15 (2, 219 QFZ); (bottom) $\alpha = \omega = 100$; e) original QFZ (3, 4651 QFZ); f) area threshold=5 (4, 600 QFZ); g) area threshold=10 (2, 051 QFZ); h) area threshold=15 (1, 252 QFZ).

image while the iterative area filtering keeps too many regions and may enlarge transition regions.

5.2. QFZ-based reconstruction vs. pixel-based reconstruction

We are proposing to fill removed QFZ through a QFZ-based approach rather than pixelwise. Thus we are able to keep QFZ related information and to deal with reduced data (QFZ instead of pixels). We evaluate here such a strategy, both qualitatively and computationally.

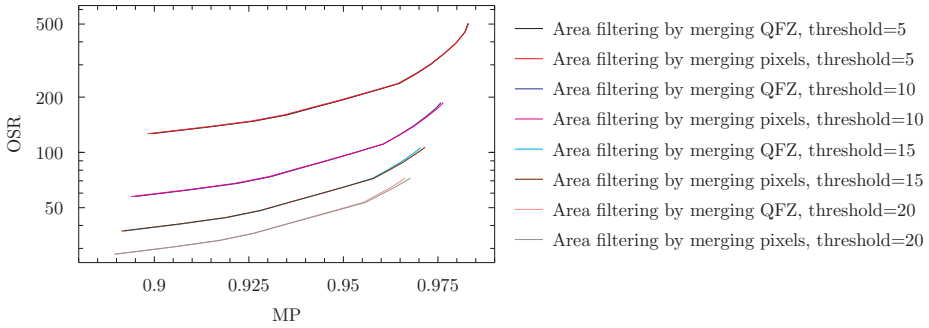

Figure 12: Comparison between filling removed QFZ using an SRG over QFZ and over pixels, using the proposed filtering approach with $C^{(\alpha,\omega)}$ on Berkeley Segmentation Dataset with different values of minimal area threshold.

In Fig. 12, we compare results obtained with both strategies. Surprisingly, we can observe that, for a given threshold value, the two strategies lead to similar quality while we would have expected the pixel-based reconstruction to be the most accurate. This is probably true for high value of the area threshold, but such values are not mandatory: indeed, a low threshold (here between 5 and 20) leads to a good trade-off between oversegmentation reduction and filtered QFZ accuracy. In such a setup, the reconstruction mainly consists of filling small holes composed of a few pixels only. Proposed strategy relying on reconstruction over QFZ is thus particularly relevant.

This observation is further strengthened when observing computation time. Indeed, we can observe, as expected, that the QFZ-based reconstruction achieves

Table 1: Average computation time comparison between filling removed QFZ using an SRG over QFZ and over pixels, using the proposed filtering approach on Berkeley Segmentation Dataset with different settings for α/ω and area threshold. Computation times correspond to a Java implementation of the algorithms performed on Intel Core i7 Q 720 CPU (1.60GHz).

α/ω	Area Thresh.	Computation time (ms)	
		QFZ-based reconstruction	Pixel-based reconstruction
50	5	**62**	126
	10	**65**	132
	15	**67**	128
	20	**69**	142
100	5	**56**	92
	10	**51**	70
	15	**51**	155
	20	**52**	160

the best results (cf. Table 1) since it operates on reduced data.

To sum up, using QFZ rather than pixels as elements on which to fill the removed QFZ has been prove to be the best strategy. It ensures a similar quality compared to pixelwise approach, while lowering the computational cost.

5.3. Area threshold selection

Our filtering approach requires a single parameter to be set, in order to define the minimal area of QFZ. While this parameter is simple and easily understandable, its setting might be far from intuitive. Moreover, it has to be set empirically since the "best" minimal area depends on the image content: a too low (resp. high) value may lead to undersegmentation (resp. oversegmentation) effects. This threshold thus depends on both image properties and user needs.

In the context of image segmentation, small details might only be extracted through a great oversegmentation. On the contrary, coarse and efficient segmentation of a wide object will require a weak oversegmentation. Setting the minimal area threshold is complex and not so intuitive.

To overcome this problem, we propose two alternative and more intuitive parameters from which we can set the minimal area threshold:

(1) Amount of remaining QFZ after filtering (similar to [6] for flat zones);
(2) Simplification ratio (i.e., percentage of QFZ to keep after filtering).

Let us note that these two parameters are linked and may be deduced one from the other:

$$\text{percentage of QFZ to keep} = \frac{\text{number of remaining QFZ}}{\text{total number of QFZ}} \tag{5}$$

and they represent somehow a compression ratio of the QFZ partition.

The minimal area threshold is set to the highest area which satisfies the constraint (e.g., number of remaining QFZ).

These parameters are more intuitive to set for a user and do not depend anymore on the image spatial resolution. Nevertheless, an automatic setting is still hardly achievable, while the optimal threshold is related to the user goal and the image content. Furthermore, the need of keeping small details may lead to very small area threshold values (thus lowering the impact of the proposed approach). However, we have not observed such a need on real scenarios where most often details remain after filtering. To illustrate, Fig. 13 shows the detail conservation even with relatively high area threshold values. We can also observe that the segmentation quality is more sensitive to α/ω than to the area threshold. Our filtering method only filters transition regions, isolated pixel and very small QFZ. Image details (even as small as *Lenna*'s eyes) are too large to be filtered. In practice, selecting a area threshold value between 10 and 20 lead to satisfying results since it ensures an important oversegmentation reduction while keeping important details such as *Lenna*'s eyes.

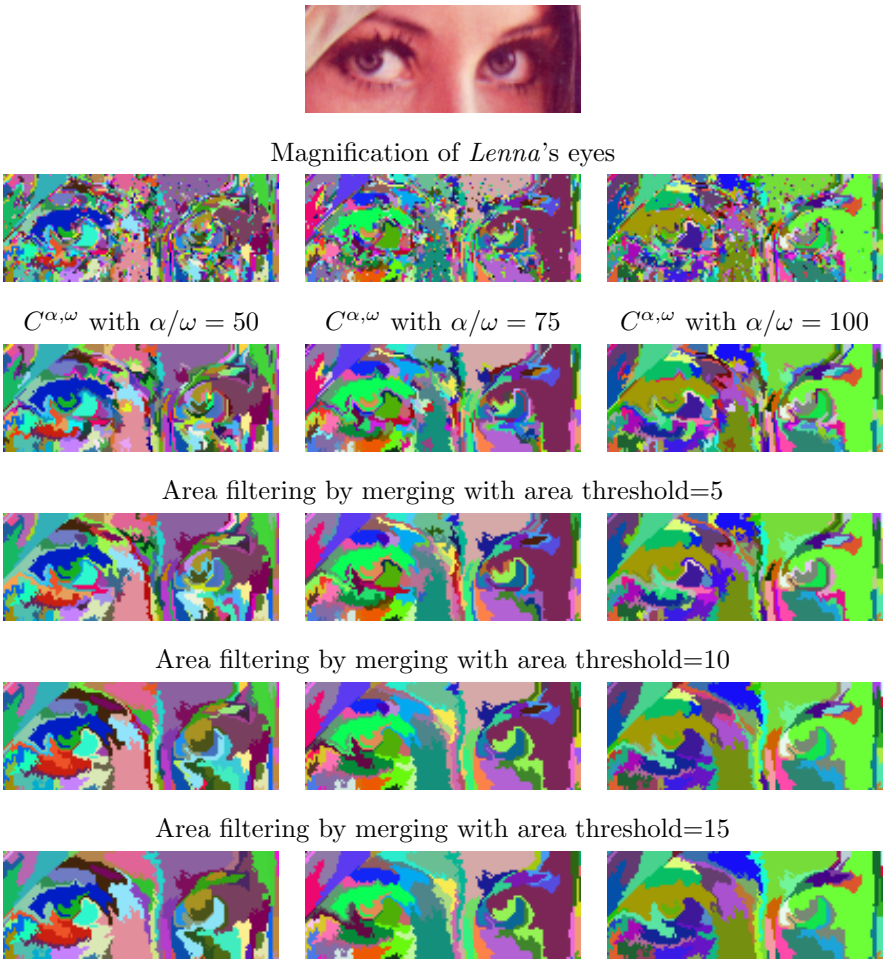

Figure 13: Illustration of detail conservation with the example of Lenna's eyes and different area threshold and α/ω values.

5.4. Discussion

Existing approaches suffer from several drawbacks: (1) enlargement of transition regions, (2) inability to remove small QFZ, (3) spatial shift of edges, (4) loss of QFZ information, and (5) parameter settings. In Tab. 2, we provide a survey of the state-of-the-art (including also our contribution) w.r.t. these drawbacks. It clearly shows that the only drawback of our approach is the need of parameter settings, while other methods face more cons. Indeed, transition regions are not enlarged with our method since QFZ removal is not an iterative process based on threshold area incrementation. Moreover, small QFZ made of few pixels are not kept as all QFZ smaller than the area threshold are removed. Furthermore, image edges are not shifted since we rely on QFZ edges, which are part of image edges. Finally, our method performs the reconstruction process on QFZ rather than pixels, ensuring thus to keeps QFZ-related information.

Drawbacks	Methods					
	[14]	[13]	[2]	[17]	[4]	**Ours**
Enlargement of transition regions			X		X	
Inability to remove small QFZ	X	X				
Spatial shift of edges		X				
Loss of QFZ information	X			X	X	
Parameter settings			X	X	X	**X**

Table 2: Qualitative analysis of QFZ filtering methods.

Besides having less drawbacks, our approach also presents some great advantages. Indeed, performing the reconstruction on QFZ rather than pixelwise leads to a strong decrease of the computation time. This does not come with a lower quality of the resulting QFZ. This property is of first importance in the context of image segmentation, as it will be shown in the next section.

6. Experiments

To evaluate the effectiveness of our filtering approach, we performed an extended experimental comparison with related work, following the protocol given in Sec. 3.

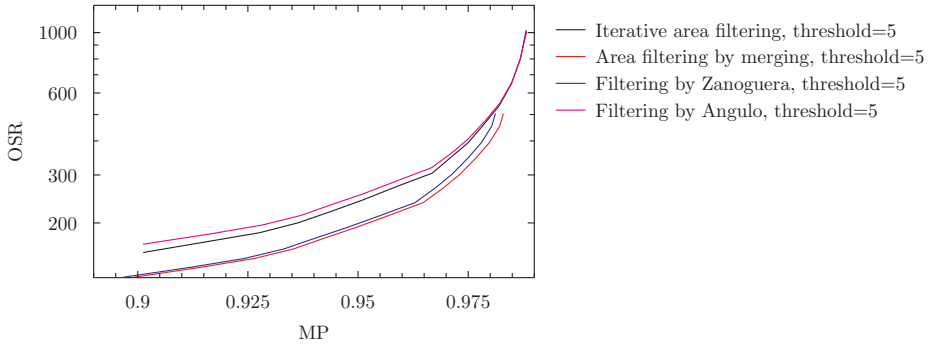

Figure 14: Comparison of our approach (area filtering by merging) and existing filtering methods based on an area threshold using $C^{\alpha,\omega}$ on the Berkeley Dataset.

Since parametric approaches have been shown to provide the best results among existing filtering methods (Fig. 8), we consider them as a fair representative of the state-of-the-art. The quantitative evaluation using MP and OSR on the whole Berkeley dataset is given in Fig. 14 and some qualitative results are shown in Fig. 15 for a visual evaluation. We can observe that, for a given level of precision, our method is able to achieve greatest oversegmentation reduction. Nevertheless, the quality is only slightly better than with Zanoguera's approach, and our method fails to achieve highest levels of precision. This might be explained by the fact that our method does not modify QFZ boundaries, while iterative area filtering is able to correct them by filling the removed QFZ on a pixel basis. Nevertheless, assuming initial QFZ ensure sufficient accuracy, our approach greatly decreases the computational cost by working on the QFZ rather than on the pixels. Furthermore, it is not based on an iterative merging process like Angulo's approach (having a higher precision but also a higher oversegmentation).

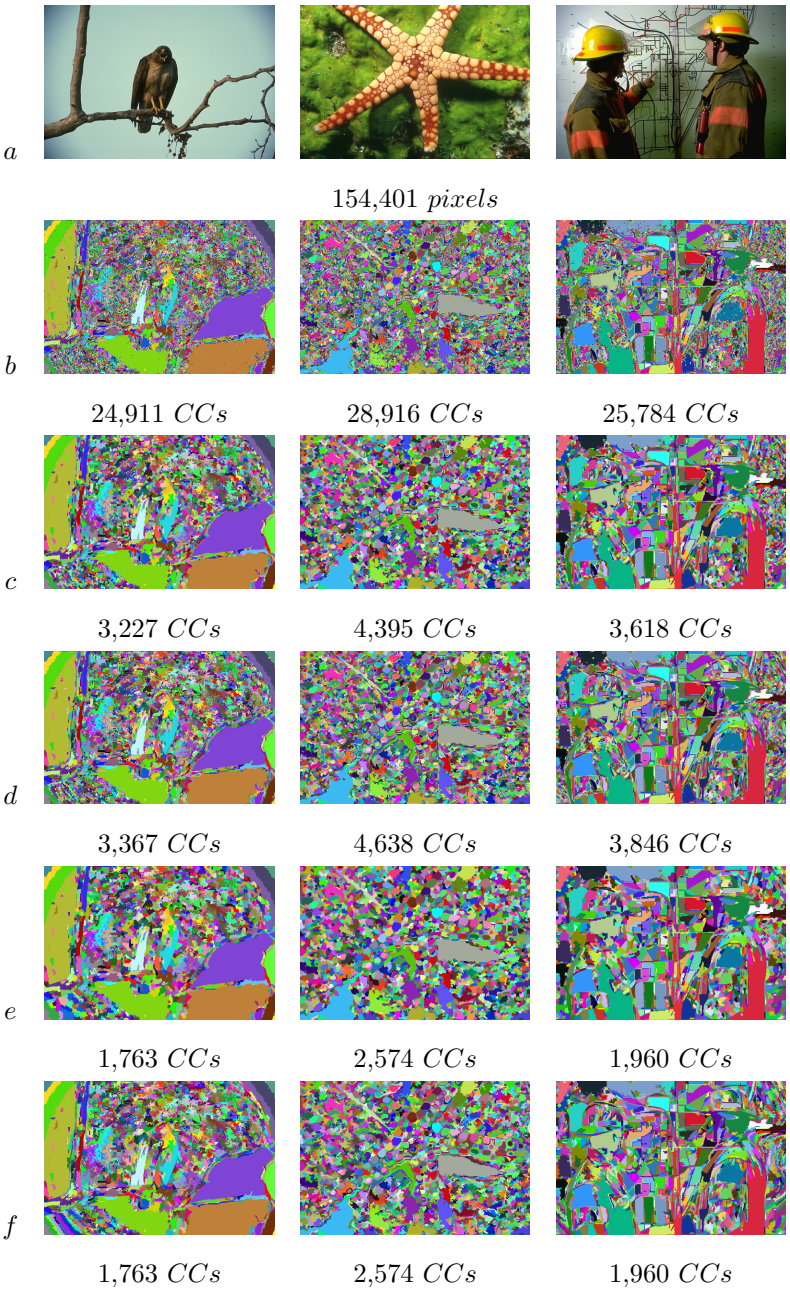

Figure 15: Visual illustration of results obtained by parametric approaches using $C^{\alpha,\omega}$ on the Berkeley Dataset with $\alpha/\omega = 50$ and an area threshold=10. a) original image ; b) unfiltered QFZ ; c) iterative area filtering ; d) Angulo's approach ; e) Zanoguera's approach, f) area filtering by merging (proposed approach)

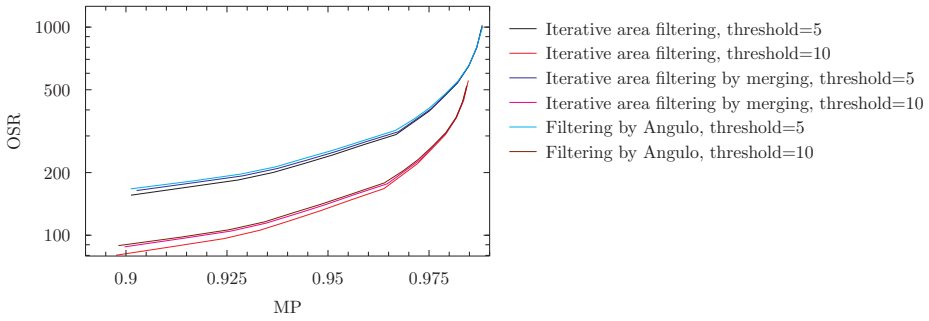

Figure 16: Comparison of the iterative version of our approach, iterative area filtering and Angulo's approach with $C^{\alpha,\omega}$ on the Berkeley Dataset.

In order to achieve a fully fair comparison with iterative approaches, we also designed an iterative version of the proposed filtering approach. Results are given in Fig. 16 and show a similar behavior with the two existing iterative approaches (Iterative area filtering and Angulo's method). Thus, applying the SRG on QFZ instead of pixels does not significantly influence the result quality while lowering the computation time (cf. Tab. 3). We can conclude that our approach and its iterative version are more relevant than the existing iterative filtering methods. We nevertheless suggest the use of the non-iterative definition, since it makes possible to work on reduced data (cf. Fig. 14 and Fig. 16) and thus comes with a lower computational cost (cf. Tab. 3).

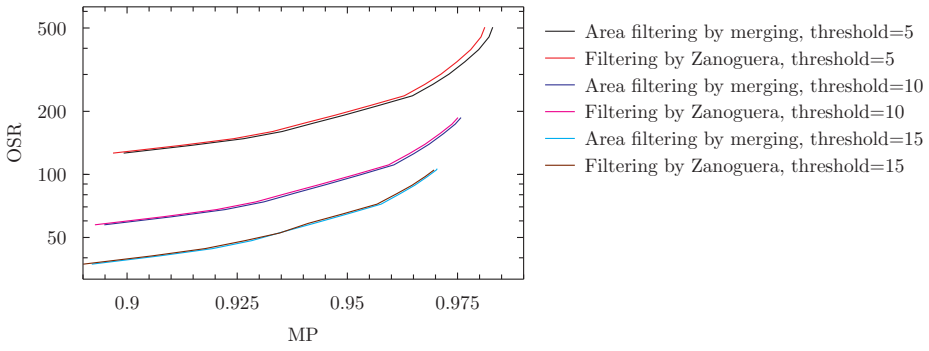

Figure 17: Comparison of our approach and Zanoguera's approach with $C^{\alpha,\omega}$ on the Berkeley Dataset.

Zanoguera's filtering method has been shown to provide only slightly lower results when compared to our method. So, we further compare these two methods using different threshold values, see Fig. 17. We can observe that our approach always comes first, but the difference becomes negligible when the threshold value increases. Still, computational complexity stays an advantage of our method when compared to Zanoguera's (cf. Tab. 3).

Table 3: Comparison of average computation times obtained for Berkeley dataset images, with the proposed approach, its iterative version and the parametric existing approaches through different combinations of α/ω and area threshold. Computation times correspond to a Java implementation of the algorithms performed on Intel Core i7 Q 720 CPU (1.60GHz).

α/ω	Min area	Computation time (ms)				
		Proposed	Iterative Area Filt.	Zanoguera	Angulo	Proposed (iterative)
50	5	**62**	292	160	131	199
	10	**65**	368	165	188	202
	15	**67**	448	123	190	291
	20	**69**	519	146	189	379
100	5	**56**	285	112	161	92
	10	**51**	347	109	190	175
	15	**51**	400	135	189	250
	20	**52**	469	140	194	329

The experimental evaluation and comparisons with state-of-the-art approaches described in this section support the relevance of our contribution which outperforms existing approaches (both from a quality and computation point-of-view).

While we aim in this paper to introduce a new QFZ filtering method and to

Figure 18: QFZ-based video segmentation on a sample frame of the *carphone* video sequence: a) Original frame, b) Markers provided by the user, c) QFZ ($\alpha = \omega = 50$), d) Filtered QFZ (area threshold=20), e) Segmentation result using QFZ, f) Segmentation result using filtered QFZ

show how it outperforms related work, we also illustrate the relevance of this approach in the context of image segmentation. To do so, we rely on previous works [15, 16] where interactive video segmentation has been achieved using filtered QFZ as a pre-segmentation step, leading to better results while decreasing the computation time. Fig. 18 illustrates the relevance of QFZ filtering in the context of QFZ-based interactive segmentation. While QFZ filtering only slightly improve the visual quality of the segmentation, it has a great impact on the overall computation time. Indeed, the segmentation process requires $9,401$ ms when operating on the whole set of QFZ, but only 150 ms if filtered QFZ are considered. This is of course due to the strong reduction in the amount of QFZ, from $432,596$ QFZ before filtering to $6,316$ after. Moreover, we also compare QFZ-based and filtered QFZ-based segmentation on the Berkeley segmentation dataset. Sample results are provided in Fig. 19 and confirm on still images

the conclusions driven from segmentation on video sequences. Using filtered QFZ leads to results of similar (or slightly better) quality but greatly decreases the computation time as already indicated. Within an interactive segmentation framework, the computation time required by the segmentation process is of first importance. Thus the filtering method proposed in this paper is of high interest in this context.

The QFZ filtering step also brings some noise robustness to QFZ, which are critically sensitive to such artifcats. In fact, the QFZ parameter α is defined as a local difference between pixel values. Such kind of distance is very sensitive to noise, especially to *salt & pepper* noise. *Salt & pepper* noise induces local extrema composed of isolated pixels, which are completely filtered by our approach. Fig. 20 illustrates this advantage and also shows a comparison of interactive segmentations of a noisy image when relying on initial vs. filtered QFZ. As expected, many small QFZ are produced from the noisy image ($25,842$ QFZ). They are all filtered by our approach, leading to a very low number of QFZ (179 QFZ). Moreover, the interactive segmentation based on the filtered QFZ is faster (14 ms vs. 448 ms) and more accurate than the one based on unfiltered QFZ. Indeed, in the image of Fig. 20, the tallest tree is not correctly segmented using the QFZ, due to noise effects, while it is correctly segmented using filtered QFZ. This example illustrates the relevance of our filtering approach in the presence of noise, allowing in such a case the QFZ-based interactive segmentation process to achieve better results.

7. Conclusion

QFZ are connected sets of homogeneous pixels, which might be further aggregated to achieve image simplification or image segmentation. However, all QFZ definitions inherently lead to oversegmentation effects. While several filtering methods have been proposed in the literature to tackle this problem, none of them has be shown totally satisfying. Thus we have proposed in this paper

a new QFZ filtering method based on an area threshold removing small QFZ, followed by a filling of removed parts by remaining QFZ. A way to intuitively set the area threshold as a compression ratio has also been introduced. Finally, an experimental comparison with the state-of-the-art has been performed to highlight the relevance of our proposal.

Future works will focus on the metrics used to merge the QFZ in the SRG step. Furthermore, we currently select the QFZ to be removed using an area criterion. In some cases, one might want to remove large QFZ while keeping some small ones. A deeper study on possible criteria will improve the filtering process and allows to reduce more efficiently the oversegmentation without loss of accuracy.

References

[1] Adams, R., Bischof, L., 1994. Seeded region growing. IEEE Transactions on Pattern Analysis and Machine Intelligence 16 (6), 641–647.

[2] Angulo, J., 2003. Morphologie mathématique et indexation d'images couleur. application à la microscopie en biomédecine. Ph.D. thesis, Ecole des Mines de Paris.

[3] Angulo, J., Serra, J., 2003. Color segmentation by ordered mergings. In: Proceedings of the IEEE International Conference on Image Processing. pp. 125–128.

[4] Brunner, D., Soille, P., 2007. Iterative area filtering of multichannel images. Image and Vision Computing 25 (8), 1352–1364.

[5] Carleer, A., Debeir, O., Wolff, E., November 2005. Assessment of very high spatial resolution satellite image segmentations. Photogrammetric Engineering & Remote Sensing 71 (11), 1285–1294.

[6] Crespo, J., Schafer, R., Serra, J., Gratin, C., Meyer, F., 1997. The flat zone approach: a general low-level region merging segmentation method. Signal Processing 62 (1), 37–60.

[7] Derivaux, S., Forestier, G., Wemmert, C., Lefèvre, S., 2010. Supervised image segmentation using watershed transform, fuzzy classification and evolutionary computation. Pattern Recognition Letters 31 (15), 2364–2374.

[8] Martin, D., Fowlkes, C., Tal, D., Malik, J., 2001. A database of human segmented natural images and its application to evaluating segmentation algorithms and measuring ecological statistics. In: Proceedings of the 8th International Conference on Computer Vision. Vol. 2. Vancouver, Canada, pp. 416–425.

[9] Rivest, J.-F., Beucher, S., Delhomme, J., 1992. Marker-controlled segmentation: an application to electrical borehole imaging. Journal of Electronic Imaging 1 (2), 136–142.

[10] Serra, J., Salembier, P., 1993. Connected operators and pyramids. In: Proceedings of SPIE, Non-Linear Algebra and Morphological Image Processing,. Vol. 2030. pp. 65–76.

[11] Soille, P., 2007. On genuine connectivity relations based on logical predicates. In: International Conference on Image Analysis and Processing. pp. 487–492.

[12] Soille, P., 2008. Constrained connectivity for hierarchical image partitioning and simplification. IEEE Transactions on Pattern Analysis and Machine Intelligence 30 (7), 1132–1145.

[13] Soille, P., 2010. Constrained connectivity for the processing of very-high-resolution satellite images. International Journal of Remote Sensing 31 (22), 5879–5893.

[14] Soille, P., Grazzini, J., 2009. Constrained connectivity and transition regions. In: International Symposium on Mathematical Morphology. pp. 59–69.

[15] Weber, J., Lefèvre, S., Gançarski, P., 2011. Interactive video segmentation based on quasi-flat zones. In: International Symposium on Image and Signal Processing and Analysis (ISPA). pp. 265–270.

[16] Weber, J., Lefèvre, S., Gançarski, P., 2011. Spatio-temporal quasi-flat zones for morphological video segmentation. In: International Symposium on Mathematical Morphology. Vol. 6671. Springer-Verlag Lecture Notes in Computer Science, pp. 178–189.

[17] Zanoguera, F., 2001. Segmentation interactive d'images fixes et de séquences vidéo basée sur des hierarchies de partitions. Ph.D. thesis, Ecole des Mines de Paris.

Figure 19: QFZ-based segmentation on sample images from Berkeley Dataset. Each segmentation is provided by the initial number of QFZ and the computation time required by the marker-based segmentation.

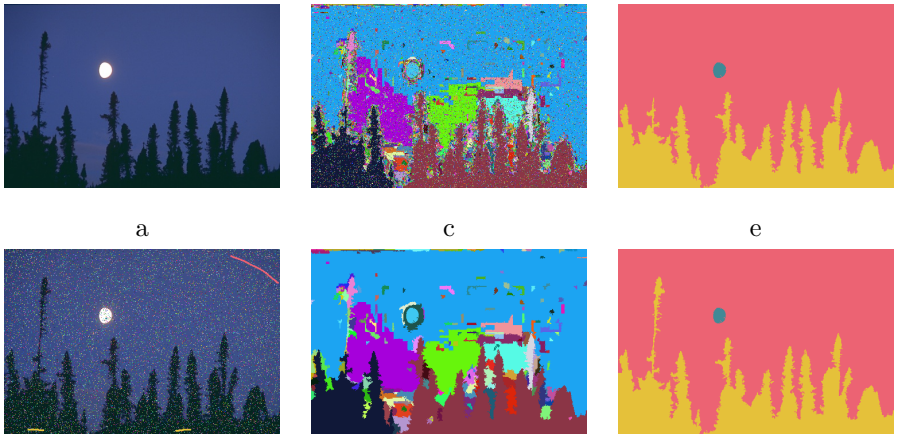

Figure 20: QFZ-based image segmentation on a noisy image: a) Original image, b) Noisy image (*salt & pepper* on 10% of pixels) with markers provided by the user, c) Unfiltered QFZ ($\alpha = \omega = 50$), d) Filtered QFZ (area threshold=20), e) Segmentation result using unfiltered QFZ, f) Segmentation result using filtered QFZ.